Chapter 11
Metal Oxide Nanowire Sensors with Complex Morphologies and Compositions

Qiuhong Li, Lin Mei, Ming Zhuo, Ming Zhang and Taihong Wang

Abstract Metal oxide nanowire sensors with complex morphologies and compositions have shown promising properties due to their high surface-to-volume ratio and stable structures against agglomeration. In this chapter, a series of metal oxide nanostructures modified via surface coating, morphology variation, doping and appropriate energy band engineering have been investigated, and the sensing mechanism is discussed. By using nanostructures with complex morphologies and compositions in simple material synthesis routes, the structure of the sensitive material is modified, the electronic transport of the sensor is regulated and the sensing properties can be greatly improved, including enhancing the sensitivity and selectivity, lowering the working temperatures, reducing the response time and achieving long-term stability.

11.1 Introduction

Metal oxide nanowire sensors have been investigated extensively in recent years [1–3]. They are promising in a wide range of applications including monitoring atmosphere quality, detecting hazardous and poisonous gases in mining or at home, diagnosing human health, among others. The metal oxide nanowires are usually *n*- or *p*-type semiconductors and sensitive to oxidizing or reducing ambient conditions. The chemical information about the ambient gas and its concentration can be turned into an electric one such as resistance, which can be easily detected [4].

Q. Li · L. Mei · M. Zhuo · M. Zhang · T. Wang (✉)
Key Laboratory for Micro-Nano Optoelectronic Devices of Ministry of Education, and State Key Laboratory for Chemo/Biosensing and Chemometrics, Hunan University, 410082 Changsha, People's Republic of China
e-mail: thwang@aphy.iphy.ac.cn

M. A. Carpenter et al. (eds.), *Metal Oxide Nanomaterials for Chemical Sensors*, Integrated Analytical Systems, DOI: 10.1007/978-1-4614-5395-6_11,

In 2004 ZnO nanowire sensors were fabricated by a MEMS technology [5]. They had shown a sensitivity of 1.9 and 47 to 1 and 200 ppm ethanol at 300 °C, respectively. The response time was about 5 s and the recovery time was about 10 s to 1 ppm ethanol. The properties were much better than thin or thick film metal oxide sensors. This high performance has attracted much attention and more different types of nanowire sensors have since been developed. Metal oxide nanowires are usually crystalline structures with well defined chemical compositions. Sensors made of these nanowires exhibit superior properties in sensitivity, selectivity, and stability due to their high surface-to-volume ratio, high degree of crystallinity and stability against agglomeration [2].

The sensors usually consist of a large number of sensitive nanostructures (when arranged in nanowire mats) that contact each other to form a thin conduction layer. As nano-sized structures, surface effects and contact barriers dominate their sensing properties, and oxygen plays an important role in their sensing mechanism. When the sensor is in air, oxygen molecules are adsorbed on the surface of the nanostructure and deprive it of electrons, forming oxygen ions (O^-, O^{2-} or $O_2{}^-$). If the sensing material is *n*-type, a depletion layer forms on the surface of the nanowire's conduction channel, and the potential barriers are built up between the nanowires, thus reducing the sensor conductance. On the other hand, for a *p*-type material, the extraction of electrons from the nanowire increases the major carrier concentration and hence increases the conductance of the sensor. Therefore, when the *n*-type sensor is put in an oxidizing gas, more electrons are deprived, the thickness of the surface depletion layer increases and the potential barriers are raised. Thus the resistance of the sensor increases. While in a reducing gas, electrons are transferred from the preadsorbed oxygen ions back to the metal oxide, the depletion layer becomes narrower, the contact barrier is reduced and the conductance of the sensor increases. With a similar mechanism, the conductance of a *p*-type sensor increases in an oxidizing gas and decreases in a reducing gas. The contact between the sensitive nanowires and electrodes may play a role as well in the transport and sensing mechanism, but it is less important than that of a single nanowire sensor since the electrodes are in parallel connection with a large number of nanostructures.

The surface depletion and contact barriers all contribute to the sensor resistance [6–8] that can be enhanced or reduced in adsorption and desorption processes, whereas which one dominates the sensing mechanism mainly depends on the size of the nanowires. If the diameter of the nanowire is much larger than the depletion width, surface depletion does not greatly affect the density and mobility of the carriers of the nanowires but significantly modifies the potential barrier of the contacts between the nanowires. When the size of nanowires is comparable to the space charge layer $2L_d$ (L_d: Debye length), surface depletion greatly affects the density and mobility of the carriers of the nanowires and these effects becomes much more dominant in the corresponding sensing mechanism. Metal oxide nanowire sensors have shown ultra high responses as the size of the nanowire is close to or smaller than $2L_d$ [8–10].

With rapidly growing demands for better sensors, sensors from simple metal oxide nanowires need to be improved and better functional sensitive materials are under development to further increase the sensitivity, quicken the response, lower the working temperature, and enhance the selectivity. Therefore, materials with complex morphologies and composition are receiving more and more attention. The addition of noble metals has been reported to improve the selectivity and stability of thin film sensors which has been adopted in nanowire sensors in the current research [11–15]. Coating or doping is proven to be an effective method to improve the sensing performance. By using coating and doping technology or fabricating sensors from hierarchical-structure nanomaterials, the contact between sensitive materials can be modified, the adsorption and desorption process can be accelerated and the sensor properties are greatly improved. The sensing properties for some nanostructures are summarized in Table 11.1.

In this chapter, a series of representative metal oxide nanostructure sensors with complex morphologies and composition are discussed, including nanoparticle and nanowire systems, hierarchical nanostructures, metal doping in nanowires, and multiple-composition oxide nanowires. We demonstrate that the sensor properties such as sensitivity, selectivity, response time and stability can be greatly improved via the aforementioned methods.

11.2 Sensors Packaging and Measurement Setup

The sensors in this chapter are fabricated in a commercial style as shown in Fig. 11.1a. After material synthesis they are usually dispersed in a solution such as water or ethanol to get homogenous paste for coating on a ceramic tube. As shown in Fig. 11.1a, a ceramic tube is welded on a six-electrode basic stand to connect with an outside electronic circuit. The tube has a diameter of 1 mm and length of 5 mm. The platinum electrodes 1–4 on the surface of the ceramic tube work as measurement electrodes connecting with sensitive materials. Sensitive materials are coated on the surface of the tube to form the conductive route. Electrodes 5 and 6 are for heating and are connected with a platinum resistor located in the hollow ceramic tube center. By monitoring the voltage on the platinum resistor, the working temperature of the sensor is controlled. Before measurements the sensors are usually aging at 300 °C for 1–48 h by applying a heating voltage on the resistor.

The sensor is then connected in series with a reference resistor R_r as shown in Fig. 11.1b. As a voltage V_c (usually 5 V) is applied on the sensor and the reference resistor, the voltage on the reference resistor V_{out} can be measured and the resistance of the sensor R_s is then calculated as $R_s = (V_c - V_{out})R_r/V_{out}$. The sensor is first put in air with the resistance defined as R_s^a, and then put into a chamber in which a certain concentration of target gas mixed with air is already prepared. Then the sensor is taken out of the chamber and put in the air atmosphere again. The resistance in the detected gas is defined as R_s^g. The sensitivity (S) of the sensor is defined as $S = R_s^g/R_s^a$ as $R_s^g > R_s^a$ or $S = R_s^a/R_s^g$ as $R_s^g < R_s^a$. The real-time

Table 11.1 Sensing properties of various nanostructures to ethanol

Material	Size[a]	Sensitivity (at ethanol concentration, ppm)	Response time (s)	Working temperature (°C)	Reference
SnO_2 nanorods	4–15 nm	13.9 (100)	1	300	[39]
SnO_2 nanorods	3–12 nm	30.7 (100)	–	300	[40]
ZnO nanowires	25 ± 5 nm	32 (100) 1.9 (1)	~5	300	[5]
Flower like ZnO nanorod assembles	150 nm	14.6 (100) 2.2 (1) 1.6 (0.5)	–	300	[6]
ZnO nanorods	15 nm	29.7 (100) 4.1 (1)	–	300	[8]
Highly oriented ZnO nanorods	50 nm	100 (100)	10–100	300	[41]
In_2O_3 nanobricks	Several tens to 200 nm	~190 (100) ~10 (1)	~2	300	[7]
Branched SnO_2 Nanowires	Branch nanowires 20 nm, backbones 80 nm	50.6 (100) 2.3 (0.5)	2 4	300	[23]
SnO_2 nanobelts coated with CdS nanoparticles	Nanoparticles 10–20 nm, nanobelts 30–200 nm in width and 10–50 nm in thickness	90 (100)	~5	400	[28]
ZnO nanorods coated with CdS nanoparticles	Nanoparticles 5–12 nm, nanorods 20–40 nm	33 (100)	–	300	[42]
ZnO nanorods coated with Au nanoparticles	Nanoparticles 4 nm, nanorods 15 ± 5 nm	89.5 (100)[b] 11.3 (100)[c]	2[b] ~10[c]	300 150	[24]
Al-doped ZnO nanotetrapods	30 nm	40 (100) 5.7 (1)	–	300	[43]
In-doped ZnO nanowires	60–150 nm	27 (100) 3 (1)	2	300	[44]
In-doped SnO_2 (ITO) nanowires	70–150 nm	40 (200)	2	400	[35]
$ZnSnO_3$ nanowires	20–90 nm	18 (100)	1	300	[36]
SnO_2 nanorods loaded with La_2O_3	5–20 nm	213 (100)	–	200	[30]

[a] Size here represents diameter if not particularly pointed out
[b] at 300 °C
[c] at 150 °C

voltage on the reference resistor V_{out} while varying the ambient is recorded and the sensor resistance is calculated. The equipment for the sensor measurement is a highly precise sensor analyzer NS-4003 series made by China Zhong-Ke Micro-nano IOT Ltd. R_r will be chosen automatically by the equipment according to the sensor resistance. A measurement of 256 sensors can be carried out simultaneously with a time resolution of 10^{-3} s and the measurable resistance range 10^0–10^9 Ω, current range 10^{-12}–10^{-3} A, voltage range 10^{-9}–10^0 V, and capacitance range 10^{-12}–10^{-3} F. The equipment also provides accurate heating on the platinum resistor, including constant current and voltage power supply. Due to the accurate (with error less than 0.09 %) and dynamic measurement across the whole range the electric signals can be recorded precisely.

11.3 Tin Oxide Coated Multi-Walled Carbon Nanotube (MWCNT) Sensors

The sensing materials were synthesized by coating of MWCNTs with SnO_2 nanograins using an ultrasonic method [16]. The MWCNTs were prepared by an arc discharge method. The collected material was purified by reflux in H_2O_2 and then in a mixture of sulfuric and nitric acids to remove particles in the MWCNT materials. The process facilitated the formation of functional groups (mainly carboxylic acid groups) on the MWCNTs to act as sites for SnO_2 coating [17]. Such a material was sonicated in tin chloride solution with hydrochloric acid, and the resultant solution was then stirred for 30 min. Products were collected after filtration and rinsed in distilled water. High resolution transmission electron microscopy (HRTEM) studies revealed that the SnO_2 nanograins were uniformly distributed on MWCNTs with the size about 2–6 nm as shown in Fig. 11.2. Then the material was pasted on the surface of the ceramic tube for gas sensing measurement as described previously.

By changing the gas categories including NO, NO_2, C_2H_2, and ethanol with certain concentrations, the resistance was measured in real-time. The standard working temperature was about 300 °C and the resistance in air was about 130 kΩ. In oxidizing gases including NO and NO_2, the resistance increased, while in reducing gases, the sensor resistance decreased, which was in accordance with the above discussion. The sensitivity to different gases and concentrations is shown in Fig. 11.3a, b. The resistance increased to about 2.8 MΩ and 1.4 MΩ in 50 ppm of NO_2 and NO, respectively. And the resistance decreased to about 46.3 kΩ and 62.8 kΩ in 50 ppm of ethanol and C_2H_2, respectively.

The sensing performance of the SnO_2-MWCNT material can be understood in terms of the aforementioned receptor-transduction mechanism. Namely, when the sensor is in air, oxygen molecules are adsorbed on the tin oxide grains and extract electrons from them, leaving with depletion layers between the grains and thus forming barriers for electron transport. When the sensor is put in oxidizing gases

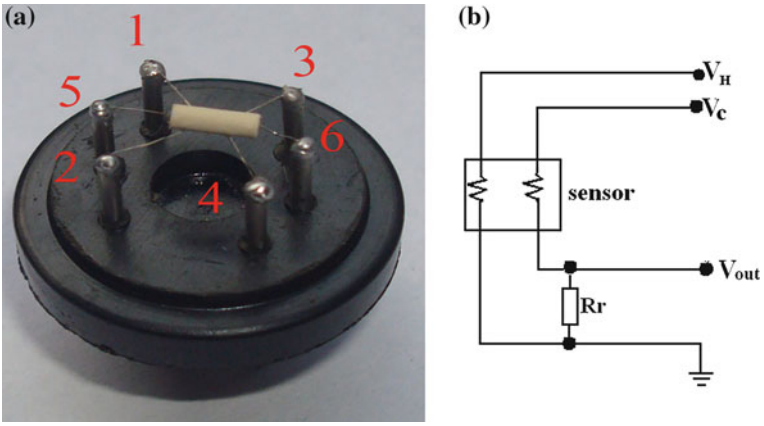

Fig. 11.1 **a** Typical photo of the sensor. *1–4* working electrodes, *5–6* heating resistor. *1* and *2* are both ends of one platinum wire, and *3* and *4* are both ends of one platinum wire. **b** Measurement circuit configuration for the sensor. V_H heating voltage, V_c voltage applied on the sensor and the reference resistor, V_{out} voltage on the reference resistor, R_r reference resistor

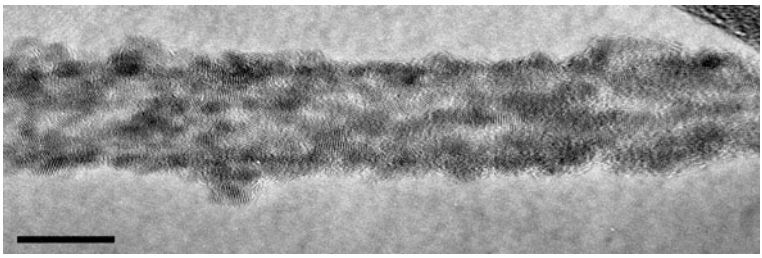

Fig. 11.2 High resolution transmission electron microscopy (*HRTEM*) image of the sensitive material for SnO_2 nanoparticle coated MWCNTs. The tin oxide nanocrystal grains can be seen clearly. *Scale bar* 10 nm

such as NO and NO_2, the molecules are directly adsorbed on SnO_2 grains and further extract electrons, so higher barriers are formed between them and the sensor resistance rises. The oxidizing response can follow the reaction path (11.1). When the sensor is taken out of the target gas and set in air again, NO_x (x: 1 or 2) gas molecules are desorbed from SnO_2 nanograins, and electrons are released. The sensor resistance then recovers. On the other hand, when the sensor is put in reducing gas such as ethanol or C_2H_2, these molecules react with preadsorbed oxygen ions and release the trapped electrons, so the barriers are lowered and the sensor resistance decreases. A representative reaction can be described as (11.2):

$$NO + e^- \rightarrow NO^- \tag{11.1}$$

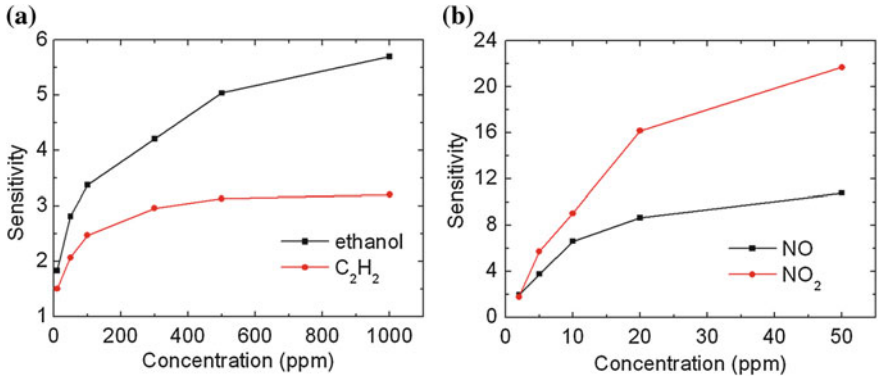

Fig. 11.3 The sensitivity in different gas concentrations for the sensors in **a** reducing gases of ethanol and C_2H_2, **b** oxidizing gases of NO and NO_2

$$C_2H_5OH + 6O^- \rightarrow 2CO_2 + 3H_2O + 6e^- \tag{11.2}$$

The sensors exhibit high selectivity to NO_x gases. SnO_2 is a typical *n*-type sensitive material and MWCNTs are highly conductive. The sensor resistance is dominated by the barriers between SnO_2 nanograins on the MWCNTs, and the barrier height is controlled by the adsorption and desorption of gas molecules, which extract or release electrons. Because the work function of the MWCNTs is approximately equal to that of SnO_2, the Schottky barrier between them is very low [18–20]. Electrons can travel through the tin oxide grains into the MWCNTs, and then conduct in MWCNTs with low resistance. The sensor exhibits rather good stability. After 3 months, the fluctuation of the sensitivity is less than ± 3 %, which indicates that the network structure of the sensor is very stable. It is assumed that MWCNTs provide a support for SnO_2 nanograins to avoid their aggregation that is a serious problem for traditional gas sensors composed of SnO_2 nanograins. The metal oxide sensors usually work at a high temperature (200–500 °C). In SnO_2 nanoparticles sensors, the nanoparticles tend to aggregate at elevated temperatures with aging that leads to structure instability [21, 22]. When the particles become larger and denser, gas diffusion into the inner part of the sensing materials becomes much more difficult. Under this configuration, a high sensitivity cannot be achieved because the resistance change occurs mostly near the surface region and the inner part remains almost inactive. Moreover, the sluggish gas diffusion through the aggregated nanostructures slows down the sensor response time.

There is another advantage of SnO_2-MWCNT system. The sensor resistance increases upon oxidizing gases. In many sensors including SnO_2 nanograins and SnO_2 thin films, the resistance is high in air. When exposed to oxidizing gases, the resistance becomes even higher (on the orders of tens or even thousands of MΩ), which is hard to measure with common circuitry. The sensors with SnO_2 nanograins

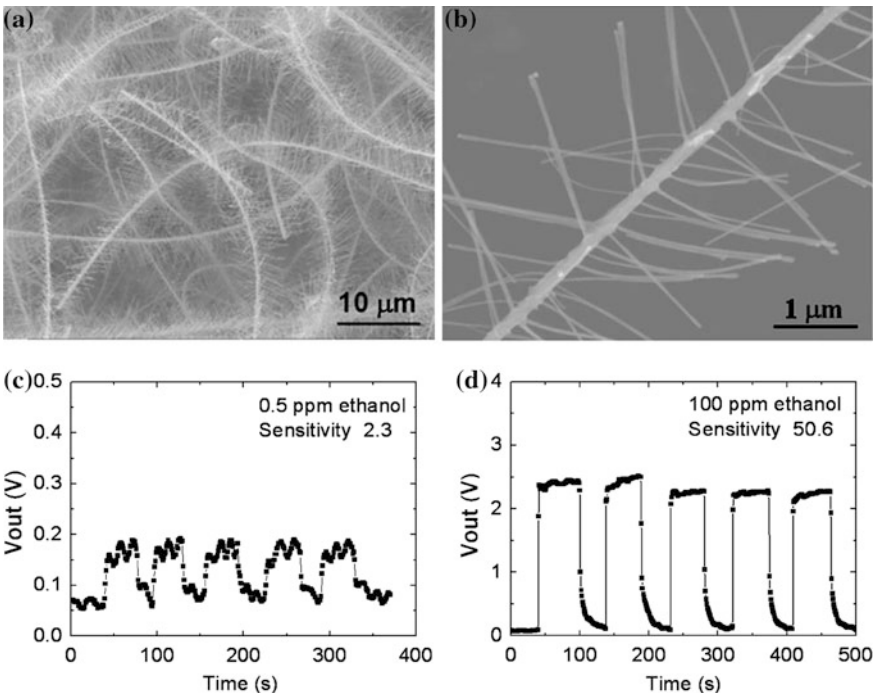

Fig. 11.4 **a** and **b** Scanning electronic microscope (*SEM*) images of the hierarchical nanostructures. Real-time response of the measured voltage on the reference resistor V_{out} as the ambient was switched between air, **c** 0.5 ppm ethanol, **d** 100 ppm ethanol (Reprinted with permission from [23], Copyright 2008, American Institute of Physics)

coated on MWCNT are in a suitable resistance range, which is favorable for the matching amplifying electronic circuit commonly available in industry.

11.4 Hierarchical Structures

With highly conductive Sb-doped SnO_2 nanowires as the backbone and SnO_2 nanowires as the branches, three dimensional hierarchical nanostructures were synthesized in a two-step vapor-liquid-solid (VLS) process [23]. Sb doped SnO_2 nanowires were first grown at 800 °C for 1 h in a furnace with Sn and Sb powders (20:1 in weight) as source materials and Au as catalyst. Then 5 nm-Au was deposited on the Sb-SnO_2 nanowires as catalyst. Similar processes were used to grow hierarchical structures with branched SnO_2 nanowires on Sb-SnO_2 nanowire backbones. The scanning electronic microscope (SEM) image of the materials is shown in Fig. 11.4a, b.

The sensors based on hierarchical nanostructures demonstrated good sensing properties as given in Fig. 11.4c, d. They could detect ethanol with the concentration as low as 0.5 ppm and the corresponding sensitivity was about 2.3. The sensitivity was 50.6–100 ppm ethanol with the response time about 2 s. The sensitivity vs. concentration showed an almost linear behavior with the concentration between 0.5 ppm and 500 ppm, which was favorable for a wide ethanol detection range.

Sensors based on hierarchical nanostructures had stable three-dimensional (3D) morphologies while maintaining the advantages of small size and high crystallinity of the nanowire structures without scarifying large surface-to-volume ratio. Owing to a large amount of porous space between the hierarchical structures in which gas molecules could diffuse quickly, the sensor had short response and recover times. Many paths for electrical conduction were offered by the branched nanowires structure with metallic backbones and high sensitivity could be achieved. The ability to detect ethanol down to 0.5 ppm level was probably related to the small size and large surface of the active SnO_2 nanowire branches. Branched SnO_2 nanowires were expected to be much more stable against agglomeration.

11.5 Nanoparticles Coated on Quasi-One Dimensional Materials

Quasi-one dimensional metal oxides, such as ZnO and SnO_2, demonstrate promising sensing properties. However, the development of high quality sensors based on the quasi-one dimensional materials still needs to be improved, including the sensitivity, response time and selectivity of the sensors. The sensors based on nanoparticles have very high surface-to-volume ratio and high sensitivity. However, since the sensor usually operates at high temperatures, nanoparticles become easily aggregated into larger size grains, which deteriorate the reliability and stability of the sensors. By combining large surface-to-volume ratio nanoparticles deposited on to the surface of stable quasi-one-dimensional crystalline nanostructures, one can expect to have better sensing performance.

11.5.1 Gold Nanoparticles Coated ZnO Nanorods

The noble metals are well known to be good catalysts. There are many reports where noble metal catalysts, including Au, Pt, Pd, and Ag have been used to improve the gas sensing properties of nanowire sensors [14, 15]. For example, Au nanoparticles are well known as active catalysts for e.g. CO oxidation, hydrogen peroxide synthesis from H_2 and O_2 and hydrocarbon oxidation. Therefore, coating nanowires with Au nanoparticles is an effective way to improve the gas sensing properties of metal oxide nanostructures.

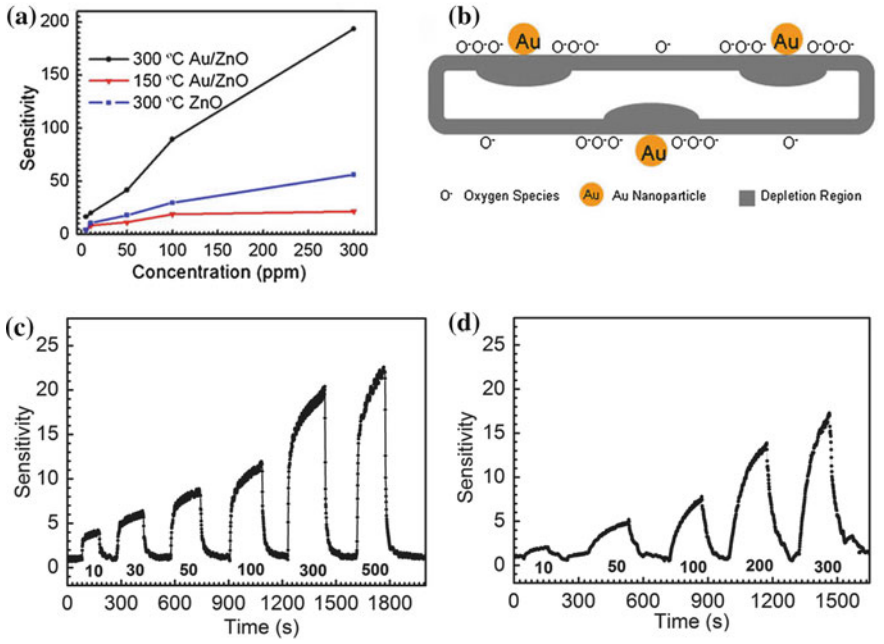

Fig. 11.5 **a** Sensitivity of the sensor to different ethanol concentrations with/without Au nanoparticles coating at 300 and 150 °C, **b** illustrations of chemical sensitization of the Au coated nanorods, and real-time response of the nanorod, **c** with and **d** without Au nanoparticle coating to different ethanol concentrations at 150 °C. The concentration of ethanol is indicated in **c** and **d**

ZnO nanorods were first pasted on the ceramic tubes and then Au nanoparticles were deposited on the nanorods by sputtering [24]. The sensors were annealed at 700 °C in a muffle furnace for 1 h before measurement. The average diameter and length of the nanorods were about 15 nm and 1 μm, respectively, and the diameter of Au nanoparticles was about 4 nm. Figure 11.5a, c, and d show comparatively the performance of the sensor with respect to various ethanol concentrations at 150 and 300 °C with or without Au nanoparticle coating. The sensitivity of ZnO nanorods functionalized with Au nanoparticles could reach 89.5 to 100 ppm ethanol with a response time of less than 2 s at 300 °C. Moreover, the sensor with Au nanoparticle coating could work at low temperatures, specifically the sensitivity to 100 ppm ethanol was 11.3 even as the working temperature was lowered down to 150 °C, and the response and recovery times of the sensors at 150 °C were only about 10 and 20 s, respectively. On the contrary, for the sensors without Au nanoparticle coating, the sensitivity to 100 ppm ethanol was 7, and the response and recovery times were about 80 and 55 s, respectively, which are longer than the sensors with Au nanoparticle coating.

Compared with bare ZnO nanorods, the sensing properties were greatly improved not only in sensitivity but also in response time, which could be related to the increasing rate of oxygen adsorption and desorption due to the catalytic

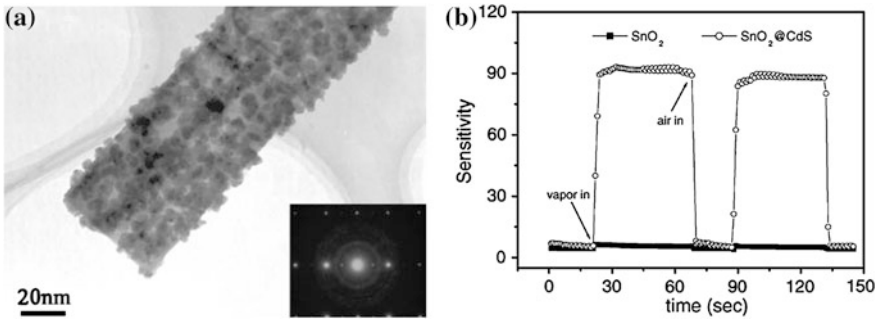

Fig. 11.6 **a** Typical transmission electron microscopy (*TEM*) image of the SnO_2 nanobelt coated with CdS, and the inset shows the corresponding selected area electron diffraction (*SAED*) patterns, **b** Response curves of the SnO_2-nanobelt and the CdS-nanoparticle-coated-SnO_2-nanobelt sensors to 100 ppm ethanolethanol at 400 °C (Reprinted with permission from [28], Copyright 2004, The Royal Society of Chemistry)

action of Au nanoparticles. As shown in Fig. 11.5b, Au nanoparticles activate the oxygen molecules, which could be more easily adsorbed on the surface of ZnO nanorods. This adsorbed oxygen could diffuse faster to surface vacancies and capture electrons from the conduction band of ZnO nanorods to become oxygen ions (O^-, O^{2-} or O_2^-). This catalyst decreases the working temperature of the sensor and increases the quantity of adsorbed oxygen. The latter results in greater and faster degree of ZnO nanorods electron depletion, which in turn defines its higher sensitivity and faster response. With reduction of the size of Au particles, the chemical sensitization effect of nanomaterials becomes much more remarkable and the working temperature could be lowered further [25–27]. These sensors demonstrated promising characteristics, especially on their low working temperatures, which could be related to Au activation and small size effect. The method provides an easy way to enhance the sensor performance.

11.5.2 SnO_2 Nanobelts Functionalized with CdS Nanoparticles

The sensing materials composed of CdS nanoparticles decorating SnO_2 nanobelts were prepared by a sonochemical synthesis method [28]. First, single crystalline SnO_2 nanobelts with 30–200 nm in width, 10–50 nm in thickness, and several hundreds of microns in length were prepared by a thermal evaporation of Sn powders at 800 °C. Then they were mixed in water with cadmium chloride and thiourea in a sonication cell. The mixture was subjected to high-intensity ultrasonication for 1–3 h. After sonication the excess CdS nanoparticles were separated from the rest of the mixture by centrifugation. Then the products were washed, centrifuged and dried. The CdS nanoparticles were nearly spherical and had

typical diameters in the range of 10–20 nm. The typical transmission electron microscopy (TEM) image of the coated SnO_2 nanobelt was shown in Fig. 11.6a.

The SnO_2 nanobelt/CdS nanoparticle sensor had a high sensitivity to 100 ppm ethanol (about 90) in air at 400 °C. As shown in Fig. 11.6b, the sensitivity of the coated structure was much higher than that of uncoated nanobelts.

As we know, SnO_2 is a wide bandgap semiconductor with Eg = 3.6 eV, and CdS is a narrow one with Eg = 2.4 eV. The energy band diagram of SnO_2 and CdS heterostructures indicates that electrons would be transported from the coated CdS nanoparticles to the SnO_2 nanobelts in a thermal equilibrium. An accumulation layer of electrons is formed in the interface of SnO_2/CdS. Thus, compared with pristine SnO_2 nanobelts, the heterojunction offers an additional source for electrons, that is, the CdS nanoparticles. Compared with general SnO_2 nanoparticles and thin films, the sensor has a lower resistance about 16 kΩ. In combination with the large surface-to-volume ratio of CdS nanoparticles and stable nature of SnO_2 nanobelts, the sensors are expected to have high sensitivity and to be more stable. Other than the noble metal addition, CdS coating is a good way to improve gas sensing properties toward specific gases.

11.5.3 p–n Junctions at the Interface Between CuO Nanoparticles and SnO_2 Nanorods

Band engineering is a very effective approach not only for microelectronic devices but also for semiconductor sensors. As an example, by using the *p–n* junction in CuO-SnO_2 nanostructures, we show that such sensors demonstrate ultra high sensitivity and selectivity when exposed to H_2S even at room temperature [29]. CuO and SnO_2 are known to be a *p*-type and *n*- type semiconductors, respectively. Nanoscale *p–n* junctions were formed by coating SnO_2 nanorods with CuO nanoparticles. The SnO_2 nanorods were synthesized by a hydrothermal method, with a typical diameter and length of 10 and 100 nm, respectively. They were added in ethanol solution with $Cu(NO_3)_2$. $3H_2O$. After ultrasonic and stirring treatment, green products were collected, filtered and dried at 75 °C. Then the products were annealed with a slowly rising temperature to 800 °C and the final materials with CuO nanoparticles coated on SnO_2 nanorods were finally collected. TEM inspection revealed that CuO nanoparticles had an average diameter about 4 nm.

The gas sensing properties of this material were tested at 18, 60, 95, 180, and 300 °C and the sensitivity to 10 ppm H_2S was shown in Fig. 11.7a. It could be as high as 9.4×10^4 at 60 °C. The response time was about 30 s and the recovery time lasted several hours at 60 °C. Raising the working temperature could shorten both the recovery and response time in a large degree, but the sensitivity also decreased with elevating temperatures. When the temperature rose above 103 °C, CuS converted into Cu_2S with lower conductivity, resulting in a decrease of sensitivity with increasing temperatures. Also, the sensing properties to different gases including

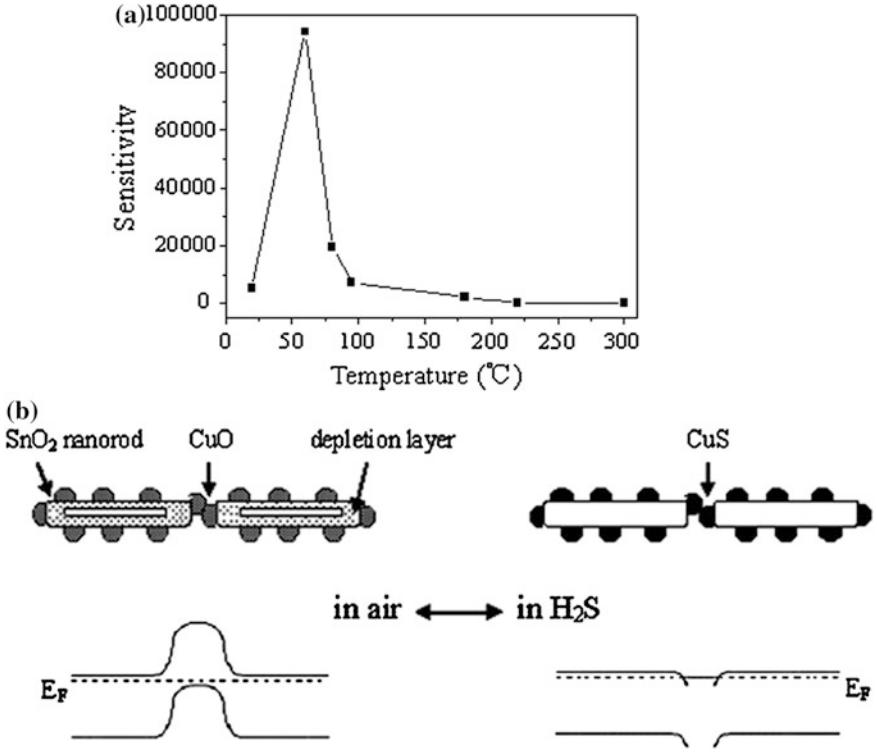

Fig. 11.7 **a** Sensitivity of the sensor at different temperatures to 10 ppm H_2S, **b** energy band diagram illustration of the CuO-SnO_2 PN junction sensor to H_2S gas (Reprinted with permission from [29], Copyright 2008, American Chemical Society)

ethanol, SO_2, and H_2 had been investigated, and the sensitivity toward these gases was found to be more than 1 order of magnitude smaller at room temperature. Such good selectivity toward H_2S can be used to avoid the interference of other gases.

The good performance in sensitivity and selectivity could be explained by the presence of the p–n junction and small size effect. *P-type* CuO nanoparticles were coated on *n*- type SnO_2 nanorods uniformly along the rods, forming the network of *p–n* junctions at the surface of the nanorod as shown in Fig. 11.7b [29]. When the sensor was in air, the barriers at the junctions effectively blocked the electrons flowing through the nanorods, resulting in a very low conductance. On the other hand, when the sensor was exposed to H_2S gas, the CuO nanoparticles reacted with H_2S following the chemical reaction:

$$CuO + H_2S \rightarrow CuS + H_2O \tag{11.3}$$

CuS was reported to have relatively high metal-like conductivity. Upon the reaction (11.3) *p–n* barriers disappeared. Since the work function of CuS is lower than that of SnO_2 as shown in Fig. 11.7b, the conductance of the sensing material become greatly

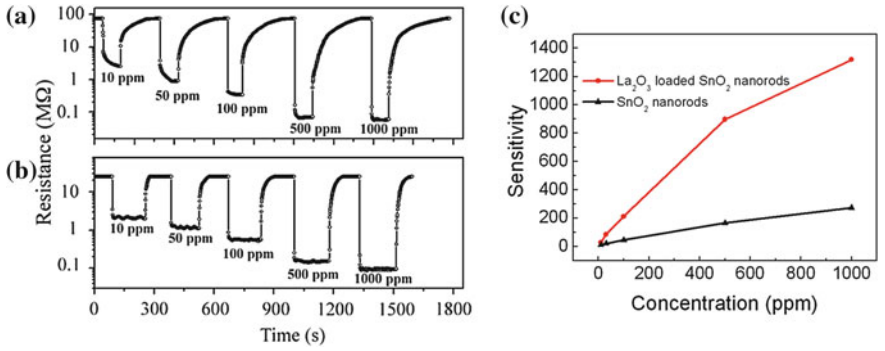

Fig. 11.8 Real-time resistance of the SnO_2 nanorod sensors **a** with and **b** without La_2O_3 loading to different concentrations of ethanolethanol (Reprinted with permission from [30], Copyright 2009, Elsevier). **c** Sensitivity of the sensor at different ethanol concentrations with and without La_2O_3 loading

enhanced. In addition to the reduction reaction with CuO, H_2S being a reducing agent, also reduced pre-adsorbed oxygen that increased the conductance further. Taking into consideration the comparability of the diameter of SnO_2 nanorods to the depletion width one can assume the conduction channel inside the nanorods could be very narrow and the resistance in air could be very large. As a result, a large resistance change could be observed upon exposure of the sensor to H_2S, which implied a super high sensitivity as large as 10^4. Moreover, the reaction in (11.3) was effective for H_2S gas but not for H_2, ethanol or SO_2, therefore a high selectivity to H_2S was achieved.

11.5.4 La_2O_3 Loaded SnO_2 Nanorods

Another example of the surface functionalization of nanowire sensors is SnO_2 nanorods loaded with La_2O_3. SnO_2 nanorods with diameters about 5–20 nm and length about 100–200 nm were synthesized by a hydrothermal method [30]. After dropping $La(NO_3)_3{\cdot}6H_2O$ into SnO_2 nanorod solutions, stirring for 4 h, and annealing the materials at 800 °C for 3 h, $La(NO_3)_3$ was converted into La_2O_3, and the La_2O_3 loaded SnO_2 nanorods were obtained.

The response of SnO_2 nanorod sensors with/without 5 % weight La_2O_3 towards ethanol gas at a working temperature of 200 °C is shown in Fig. 11.8a, b, respectively, and the sensitivity vs. concentration was shown in Fig. 11.8c. The sensitivity was 213 to 100 ppm ethanol. As the temperature increased, the sensitivity became smaller due to the decrease of resistance in air with increasing temperature, closely related to a thermally activation mechanism.

The high performance of the sensor can be interpreted by taking into account the surface chemical properties of these two oxides. Generally the sensing mechanism is based on the change of resistance when exposed to ethanol that reacts with the

adsorbed oxygen species followed reaction (11.2) discussed above. The ethanol molecules become oxidized to CO_2 and H_2O. The reaction transfers electrons back to the conduction band, and as a result the resistance of the sensors decreases. Interactions of ethanol molecules with the oxide surfaces are quite complicated and the sensor signal depends both on the density and nature of surface active centers. Depending on the surface chemical conditions of oxides, the ethanol molecules can convert to CO_2 and H_2O through two kinds of reactions: (1) dehydration into C_2H_4 in the presence of acid surface groups as shown in (11.4), and (2) dehydrogenation into acetaldehyde (CH_3CHO) in the presence of basic surface groups as given in (11.5). The intermediates (C_2H_4 and CH_3CHO) then react with adsorbed oxygen ions and are turned into CO_2 and H_2O followed as (11.6) and (11.7), respectively:

$$C_2H_5OH \overset{acid-surface}{\longrightarrow} C_2H_4 + H_2O \tag{11.4}$$

$$C_2H_5OH \overset{basic-surface}{\longrightarrow} CH_3CHO + H_2 \tag{11.5}$$

$$C_2H_4 + 6O^- \rightarrow 2CO_2 + 2H_2O + 6e^- \tag{11.6}$$

$$CH_3CHO + 3O^- \rightarrow 2CO_2 + 2H_2O + 3e^- \tag{11.7}$$

The surface of the SnO_2 nanorods contains many acidic centers such as Brønsted and Lewis type [31], and ethanol molecules mainly decompose to C_2H_4 intermediates. On the other hand, La_2O_3 is a typical basic oxide [31]. Therefore, the presence of La_2O_3 at the surface of SnO_2 will reduce the amount of the acidic sites. The latter will result in the formation of Lewis acid–basic pairs, which lead to a preferred dehydrogenation process, and more ethanol molecules will convert to CH_3CHO. From the thermodynamic point of view, reaction (11.5) is more favorable than reaction (11.4) under the same conditions [32, 33], and this is the reason why SnO_2 shows a higher response to CH_3CHO than C_2H_4 with the same concentration and the La_2O_3 loading enhances the sensitivity of the SnO_2 nanorod sensor.

11.6 Doping in Oxide Nanowires and Nanowires with Multi-Compositions

Noble metal doping has a similar effect on the sensing properties to surface modification by noble metal coating that has been discussed before. The conductivity of the nanowires can be modulated by controlling the level of the doping metal, and the surface reaction path could be also modified. It is very important to control the doping level in the metal oxide nanowires during the process of their synthesis to avoid a second phase formation. To enhance the certain property of the sensor, doping with appropriate elements and levels is very promising strategy.

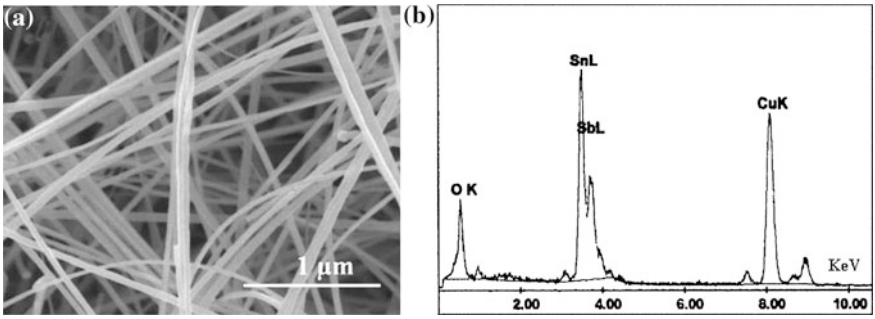

Fig. 11.9 **a** SEM image of the Sb doped SnO_2 nanowires, **b** EDS of the Sb doped SnO_2 nanowires, which inidicates the sample is composed of Sn, O and Sb (the peaks of Cu come from the Cu grids) (Reprinted with permission from [34], Copyright 2005, The Royal Society of Chemistry)

11.6.1 Sb Doped SnO_2 Nanowires

Sb doped SnO_2 nanowires were synthesized by thermal evaporation of Sn and Sb powders (the weight ratio 10:1) at 900 °C in a constant flow of 1 % oxygen and 99 % nitrogen at a rate of 5 l/min [34]. Energy dispersive X-ray spectra (EDS) revealed that the synthesized nanowires were composed of Sn, O and Sb and the atomic percentage Sb in the synthesized sample was about 3.5 %. The SEM and EDS images were shown in Fig. 11.9a, b, respectively.

The sensitivity of Sb-doped SnO_2 nanowire sensors was about 1.76 upon 10 ppm ethanol gas. The response and recovery time to 10 ppm ethanol were about 1 s and 5 s, respectively.

Sb metal doping in SnO_2 nanowires could decrease the sensor resistance in air and shorten the response and recovery time of the sensor. Presumably Sb doping accelerates the ionosorption of oxygen on the surface of the SnO_2 nanowires, which has a great significance to reduce the recovery times of the sensor.

11.6.2 Indium-Doped Tin Oxide (ITO) Nanowires and $ZnSnO_3$ Nanowires

Besides modifying the materials from accustomed binary metal oxide nanowires, new compounds composed of multiple elements such as ternary oxides have been also explored to test their sensing properties. Indium-doped tin oxide (ITO) and ZnO-SnO_2 compounds have a great potential for flexible transparent electronics, solar cells, light emitting diodes and etc. Here we briefly review their gas sensing properties.

ITO nanowires were synthesized by a thermal evaporation of In_2O_3, SnO, and graphite powders (weight ratio of 4:1:4) at 930 °C for 2 h in argon and oxygen mixed

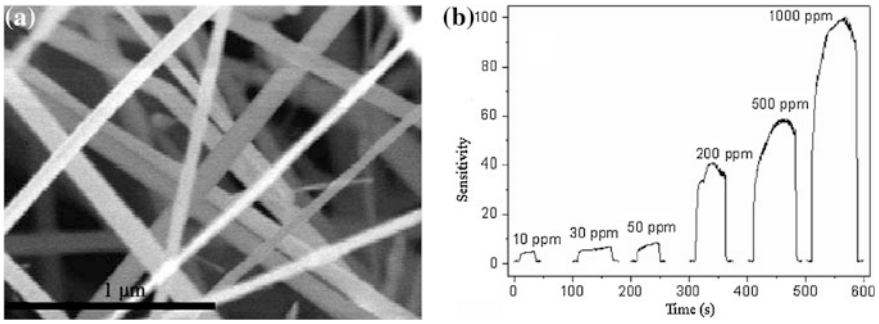

Fig. 11.10 **a** SEM image of the ITO nanowires, **b** Response of the sensor to different ethanol concentrations, insert: sketch of the nanowire in air and in ethanol (Reprinted with permission from [35], Copyright 2006, American Institute of Physics)

gases [35]. The ITO nanowires had diameters ranging from 70–150 nm and lengths of several tens of micrometers as shown in Fig. 11.10a. EDS spectrum indicated atomic ratio (In, Sn, and O) of the ITO nanowires was about 5.5: 31.6: 62.9.

The gas sensors based on ITO nanowires were very sensitive to ethanol gas as shown in Fig. 11.10b, and the sensitivity was up to 40 upon 200 ppm ethanol at 400 °C. Both the response and recovery time were less than 2 s.

$ZnSnO_3$ nanowires were synthesized by a thermal evaporation of ZnO, SnO and graphite mixture powders (weight ratio of 1:5:1) [36]. The mixture was heated to 700 °C as the pressure was kept below 4 Pa. Then a mixed gas of oxygen and argon was introduced into the tube furnace till the pressure became 1,000 Pa and the tube furnace was sealed. The mixture was heated at 990 °C for 2 h. The nanowire product was collected and analysis showed that they had a composition of $ZnSnO_3$. These nanowires had diameters ranging from 20 to 90 nm and lengths up to several tens of micrometers. EDS spectrum showed that three elements (Zn, Sn, and O) uniformly distribute over the whole nanowires, respectively.

Gas sensors based on $ZnSnO_3$ nanowires had a quick response to ethanol. The real-time response to different concentrations of ethanol at 300 °C was given in Fig. 11.11. Both response and the recovery time were about 1 s to 1 ppm ethanol. The sensitivity was about 2.7 to 1 ppm ethanol and 42 to 500 ppm ethanol, respectively.

$ZnSnO_3$ nanowires and ITO nanowires had been suggested to have higher conductivity than SnO_2 and higher sensitivity to ethanol gas than bulk ZnO, SnO_2 and Zn_2SnO_4 [37, 38]. They were potential candidates for high performance sensors and the sensing properties could also be improved by coating or doping methods in the future.

11.7 Summary

A series of metal oxide nanostructures with surface functionalization, bulk doping, and with complex morphologies or compositions are discussed and their sensing

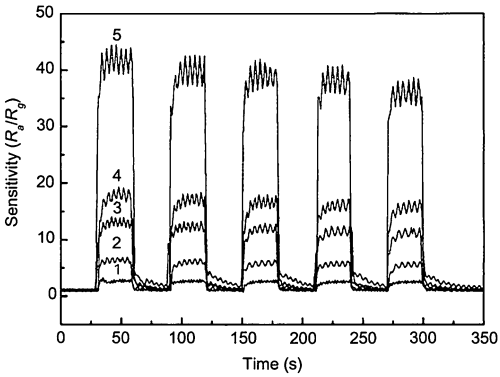

Fig. 11.11 The response of $ZnSnO_3$ nanowire sensors to ethanol at 300 °C, the curves labeled by *1–5* indicating the ethanol concentrations: 1, 10, 50, 100 and 500 ppm, respectively (Reprinted with permission from [36], Copyright 2006, American Institute of Physics)

properties along with sensing mechanisms are briefly reviewed. The nanostructure synthesis method is very simple and easy to be reproduced. It has been shown that combining the merits of functionalization, doping and morphology tuning with energy band engineering, the sensing performance of nanowires can be greatly enhanced. Among the reviewed sensors we demonstrate that the response time can be less than 1 s. The sensors exhibit high sensitivity, especially in case of SnO_2 nanorods loaded with La_2O_3 which demonstrate a sensitivity of 213 to 100 ppm ethanol even at a low working temperature of 200 °C. Alternatively very high sensitivity to H_2S has been observed for CuO-SnO_2 nanostructures which form *p–n* junctions. The selectivity of such sensors is also largely improved. The results indicate a number of guidelines to improve the sensor properties.

1. The hierarchical nanostructures possess a stable 3D morphology, and therefore provide a large amount of open space for facile gas diffusion, adsorption and desorption. In addition, the small dimension of nanostructured branches is favorable for high sensitivity. Therefore a stable, quick response and highly sensitive sensor can be achieved.
2. Nanoparticle coatings on the surfaces of quasi-one dimensional materials, nanowires/nanotubes/nanorods, provide a stable support for nanoparticles to prevent agglomeration that is usually the main reason for sensor deterioration with aging. In addition, the small nanoparticle size offers large surface-to-volume ratio and enhanced catalytic action which accounts for the high sensitivity and fast time response. Besides, noble metal doping can also performs as an effective catalyst and improve the sensor performance.
3. By choosing proper material combinations, the energy band, e.g. p–n junction, heterojunction can be engineered appropriately. All these can be used to enhance the sensitivity and selectivity of the sensors.
4. Rare earth oxides can “navigate” the intermediate reaction to a thermodynamically favorable direction that can enhance the rate of conversion of reducing gas and enhance the sensitivity of the gas sensor.

Acknowledgments The authors gratefully acknowledge the support from "973" National Key Basic Research Program of China (Grant No. 2007CB310500), National Natural Science Foundation of China (Grant No. 21003041), and Hunan Provincial Natural Science Foundation of China (Grant No.10JJ1011).

References

1. Huang XJ, Choi YK (2007) Chemical sensors based on nanostructured materials. Sens Actuators B 122:659–671
2. Comini E, Baratto C, Faglia G, Ferroni M, Vomiero A, Serveglieri G (2008) Quasi-one dimensional metal oxide semiconductors: preparation, characterization and application as chemical sensors. Prog Mater Sci 54:1–67
3. Comini E, Sberveglieri G (2010) Metal oxide nano wires as chemical sensors. Mater Today 13:36–44
4. Fraden J (2004) Handbook of modern sensors: physics, designs, and applications. Springer, New York
5. Wan Q, Li QH, Chen YJ, Wang TH (2004) Fabrication and ethanol sensing characteristics of ZnO nano wire gas sensors. Appl Phys Lett 84:3654–3656
6. Feng P, Wan Q, Wang TH (2005) Contact-controlled sensing properties of flowerlike ZnO nanostructures. Appl Phys Lett 87:213111
7. Feng P, Xue XY, Liu YG, Wang TH (2006) Highly sensitive ethanol sensors based on {100}-bounded In_2O_3 nanocrystals due to face contact. Appl Phys Lett 89:243514
8. Li CC, Du ZF, Li LM, Yu HC, Wan Q, Wang TH (2007) Surface-depletion controlled gas sensing of ZnO nano rods grown at room temperature. Appl Phys Lett 91:032101
9. Xu CN, Tamaki J, Miura N, Yamazoe N (1991) Grain size effects on gas sensitivity of porous SnO_2-based elements. Sens Actuators B 3:147–155
10. Hongsith N, Wongrat E, Kerdcharoen T, Choopun S (2010) Sensor response formula for sensor based on ZnO nanostructures. Sens Actuators B 144:67–72
11. Göpel W, Schierbaum KD (1995) SnO_2 sensors: current status and future prospects. Sens Actuators B 26:1–12
12. Yamazoe N (2005) Toward innovations of gas sensor technology. Sens Actuators B 108:2–14
13. Tien LC, Sadik PW, Norton DP, Voss LF, Pearton SJ, Wang HT, Kang BS, Ren F, Jun J, Lin J (2005) Hydrogen sensing at room temperature with Pt-coated ZnO thin films and nanorods. Appl Phys Lett 87:222106
14. Kolmakov A, Klenov DO, Lilach Y, Stemmer S, Moskovits M (2005) Enhanced gas sensing by individual SnO_2 nanowires and nanobelts functionalized with Pd catalyst particles. Nano Lett 5(4):667–673
15. Shen YB, Yamazaki T, Liu ZF, Meng D, Kikuta T (2009) Hydrogen sensors made of undoped and Pt-doped SnO_2 nanowires. J Alloy Compd 488:21–25
16. Liang YX, Chen YJ, Wang TH (2004) Low-resistance gas sensors fabricated from multiwalled carbon nanotubes coated with a thin tin oxide layer. Appl Phys Lett 85:666–668
17. Ago H, Kugler T, Cacialli F, Salaneck WR, Shaffer MSP, Windle AH, Friend RH (1999) Work functions and surface functional groups of multiwall carbon nanotubes. J Phys Chem B 103:8116
18. Sze SM (1981) Physics of semiconductor devices. Wiley, New York
19. Ago H, Kugler T, Cacialli F, Salaneck WR, Shaffer MSP, Windle AH, Friend RH (1999) Work function and surface functional groups of multiwall carbon nanotubes. J Phys Chem B 103:8116–8121
20. Sinner-Hettenbach M, Gothelid M, Wei T, Barsan N, Weimar U, Schenck HV, Giovanelli L, Lay GL (2002) Electronic structure of SnO_2(110)-4 × 1 and sputtered SnO_2(110) revealed by resonant photoemission. Surf Sci 499:85–93

21. Korotchenkov G (2005) Gas response control through structural and chemical modification of metal oxide films: state of the art and approaches. Sens Actuators B 107:209–232
22. Lee JH (2009) Gas sensors using hierarchical and hollow oxide nanostructures overview. Sens. Actuators B 140:319–336
23. Wan Q, Huang J, Xie Z, Wang TH, Dattoli EN, Lu W (2008) Branched SnO_2 nanowires on metallic nanowire backbones for ethanol sensors application. Appl Phys Lett 92:102101
24. Li CC, Li LM, Du ZF, Yu HC, Xiang YY, Li Y, Cai Y, Wang TH (2008) Rapid and ultrahigh ethanol sensing based on Au-coated ZnO nanorods. Nanotechnology 19:035501
25. Qian LH, Wang K, Li Y, Fang HT, Lu QH, Ma XL (2006) CO sensor based on Au-decorated SnO_2 nanobelt. Mater Chem Phys 100:82–84
26. Hongsith N, Viriyaworasakul C, Mangkorntong P, Mangkorntong N, Choopun S (2008) Ethanol sensor based on ZnO and Au-doped ZnO nanowires. Ceram Int 34:823–826
27. Liu XH, Zhang J, Wang LW, Yang TL, Guo XZ, Wu SH, Wang SR (2011) 3D hierarchically porous ZnO structures and their functionalization by Au nanoparticles for gas sensorsgas sensors. J Mater Chem 21:349–356
28. Gao T, Wang TH (2004) Sonochemical synthesis of SnO_2 nanobelt/CdS nanoparticle core/shell heterostructures. Chem Commun 22:2558–2559
29. Xue XY, Xing LL, Chen YJ, Shi SL, Wang YG, Wang TH (2008) Synthesis and H_2S sensing properties of CuO-SnO_2 core/shell PN-junction nanorods. J Phys Chem C 112:12157–12160
30. Shi SL, Liu YG, Chen YG, Zhang JY, Wang YG, Wang TH (2009) Ultrahigh ethanol response of SnO_2 nanorods at low working temperature arising from La_2O_3 loading. Sens Actuators B 140:426–431
31. Kovalenko VV, Zhukova AA, Rumyantseva MN, Gaskov AM, Yushchenko VV, Ivanova II, Pagnier T (2007) Surface chemistry of nanocrystalline SnO_2 effect of thermal treatment and additives. Sens Actuators B 126:52–55
32. Seiyama T, Shiokawa J, Suzuki S, Fueki K (1982) Kagaku sensa. Kodansha, Tokyo
33. Rumyantseva M, Kovalenko V, Gaskov A, Makshina E, Yuschenko V, Ivanova I, Ponzoni A, Faglia G, Comini E (2006) Nanocomposites SnO_2/Fe_2O_3: sensor and catalytic properties. Sens Actuators B 118:208–214
34. Wan Q, Wang TH (2005) Single-crystalline Sb-doped SnO_2 nanowires: synthesis and gas sensor application. Chem Commun 30:3841–3843
35. Xue XY, Chen YJ, Liu YG, Shi SL, Wang YG, Wang TH (2006) Synthesis and ethanol sensing properties of indium-doped tin oxide nanowires. Appl Phys Lett 88:201907
36. Xue XY, Chen YJ, Wang YG, Wang TH (2005) Synthesis and ethanol sensing properties of $ZnSnO_3$ nanowires. Appl Phys Lett 86:233101
37. Shen YS, Zhang TS (1993) Preparation, structure and gas-sensing properties of ultramicro $ZnSnO_3$. Sens Actuators B 12:5–9
38. Wu XH, Wang YD, Tian ZH, Liu HL, Zhou ZL, Li YF (2002) Study on $ZnSnO_3$ sensitive material based on combustible gases. Solid-State Electron 46:715–719
39. Chen YJ, Xue XY, Wang YG, Wang TH (2005) Synthesis and ethanol sensing characteristics of single crystal single crystalline SnO_2 nanorods. Appl Phys Lett 87:233503
40. Chen YJ, Nie L, Xue XY, Wang YG, Wang TH (2006) Linear ethanol sensing of SnO_2 nanorods with extremely high sensitivity. Appl Phys Lett 88:083105
41. Yang Z, Li LM, Wan Q, Liu QH, Wang TH (2008) High-performance ethanol sensing based on an aligned assembly of ZnO nanorods. Sens Actuators B 135:57–60
42. Gao T, Li QH, Wang TH (2005) Sonochemical synthesis, optical propertiesoptical properties, and electrical properties of core/shell-type ZnO nanorod/CdSCdS nanoparticle composites. Chem Mater 17:887–892
43. Li LM, Du ZF, Wang TH (2010) Enhanced sensing properties of defect-controlled ZnO nanotetrapods arising from aluminum dopingdoping. Sens Actuators B 147:165–169
44. Li LM, Li CC, Zhang J, Du ZF, Zou BS, Yu HC, Wang YG, Wang TH (2007) Bandgap narrowing and ethanol sensing properties of In-doped ZnO nanowires. Nanotechnology 18:225504